Progress In Electromagnetics Research, PIER 95, 241–266, 2009

THE OPTIMAL NUMBER AND LOCATION OF GROUNDED VIAS TO REDUCE CROSSTALK

W.-T. Huang

Department of Computer Science and Information Engineering
Minghsin University of Science and Technology
No. 1, Xinxing Rd., Xinfeng Hsinchu 30401, Taiwan, R.O.C.

C.-H. Lu and D.-B. Lin

Graduate Institute of Computer and Communication Engineering
National Taipei University of Technology
No. 1, Sec. 3, Chung-Hsiao E. Rd. Taipei 10608, Taiwan, R.O.C.

Abstract—Modern electronic products are increasingly based on high-speed, high-density circuitry operating at lower voltages. With such designs, the signal integrity (SI) in a poor printed circuit board layout is affected by noise and may become unstable. Crosstalk is a major source of noise that interferes with SI. Generally, crosstalk can be reduced by adding a guard trace between the victim and aggressor areas of the circuit. In addition, grounded vias can be added to the guard trace to help reduce crosstalk. Since a large number of grounded vias degrade the SI and reduce the flexibility of the circuit routing, we propose a method to calculate the optimal distance between grounded vias in the guard trace and determine the smallest number of vias required to achieve optimal performance in reducing crosstalk. We show by time-domain simulation that our method reduces the near-end crosstalk by 27.65% and the far-end crosstalk by more than 31.63% compared to the three-width rule. This is backed up by experimental results that show not only reductions of 34.49% and 37.55% for the near- and far-end crosstalk over time-domain, respectively, but also reductions of 2.1 dB and 3.3 dB for the near- and far-end crosstalk over the frequency-domain, respectively. Our results indicate that our method of optimal grounded vias has better performance than other methods.

Corresponding author: W.-T. Huang (wthuang@must.edu.tw).

1. INTRODUCTION

As science and technology progress, the design of digital devices and chip packages tends toward high-speed, high-density, and low-voltage operation. This makes the interconnection of traces within a printed circuit board (PCB) and among chips very difficult [1]. In high-speed operation, poor designs of interconnection traces and the coupling effect of multiple traces affect signal integrity (SI) [1, 2]. SI is a key factor in the design of a high-speed PCB [2]. Crosstalk is one major source of noise that interferes with SI. Crosstalk occurs due to the coupling effects of the mutual capacitance and inductance of two adjacent transmission lines when transient signals in one transfer energy to the other. This can disrupt normal signal operations [1, 2, 3]. Therefore, attention has increasingly focused on the SI design and layout within systems-in-package (SiPs) and PCBs [4].

One design technique for preventing crosstalk is to add a guard trace between two adjacent transmission lines designated as the victim and aggressor, whose typical topology without grounded vias is shown in Fig. 1(a) [2, 5, 6]. A guard trace is grounded by vias, which are called grounded vias [7]. Generally, the guard trace is not a transmission line. However, if the designer arbitrarily places a guard trace between the

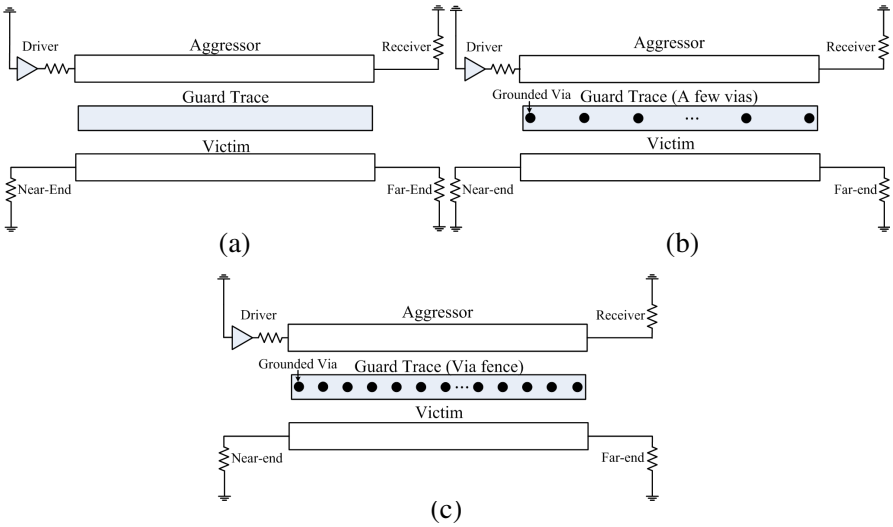

Figure 1. Three topologies with one guard trace [9]. (a) Guard trace without grounded vias. (b) Guard trace with several grounded vias. (c) Guard trace with many grounded vias (via fence).

victim and aggressor, this may aggravate the problem and cause even more crosstalk [2, 6, 8]. Therefore, adding several grounded vias in the guard trace, as shown in Fig. 1(b), will improve performance and reduce the coupling effect. In the extreme, many grounded vias can be added to the guard trace to create a via fence, as shown in Fig. 1(c) [9]. However this technique reduces the space available for the rest of the circuit layout and degrades SI [8, 10]. In addition, too many grounded vias reduce the physical strength of the PCB structure, which leads to problems in mounting components on it.

Other designs with too few grounded vias in the guard trace may not be sufficient to prevent crosstalk, and this creates a new noise source that in turn creates more crosstalk [2, 3–6]. This can also affect the signal quality in the transmission line and reduce device reliability. In this study, we present the effects of a guard trace with the optimal number of grounded vias to give the maximum effect of preventing crosstalk in parallel double microstrip lines on a high-speed PCB. Our simulation and experimental results show that our theoretical model is consistent with achieving optimal performance.

The remainder of this paper is organized as follows. Section 2 describes the principles of our basic model and Section 3 discusses the reference test board topology. Sections 4 and 5 describe our simulation and experimental results, respectively. Section 6 contains the discussion of our simulation and measurement results. Section 7 presents our conclusions.

2. CROSSTALK

Crosstalk is a noise source in PCBs that interferes with SI, and is of particular concern in high-density and high-speed circuits. It occurs due to the coupling effects caused by the mutual capacitance (C_m) and mutual inductance (L_m) of the victim and aggressor, driven by the transient signals in the aggressor. The equivalent model of a pair of transmission lines is shown in Fig. 2 [1]. The end of the victim closest to the driver (receiver) of the aggressor is called the near (far) end. When the rise and fall times of the aggressor's transient logic states change continually, the signal operation of the victim will be destroyed since the coupling effect of C_m and L_m transfer energy from the aggressor [1]. Since modern high-density circuits have high C_m and L_m, crosstalk noise is a major cause of concern in system design.

When crosstalk occurs between two adjacent transmission lines used to transmit or receive electrical signals between neighboring components, two types of crosstalk will be formed at the near and far ends of the victim. Fig. 3(a) shows a typical crosstalk signature of

a victim without a guard trace [2, 6]. Since the victim transmission line has the same impedance as the aggressor transmission line, crosstalk is transferred in the near- and far-end directions at the same energy but in opposite directions; these are referred to as $v_{b(i)}$ and $v_{f(i)}$ in Fig. 3(b), where $1 \leq i \leq n$ is the unit propagation time delay (TD) [2]. Therefore, this resulting crosstalk can be divided into near-end crosstalk ($NEXT$) and far-end crosstalk ($FEXT$) in the victim, whose typical diagram is shown in Fig. 3(a) [2]. $NEXT$ is defined as crosstalk seen in the victim nearest the driver, and $FEXT$ is defined as crosstalk observed in the victim farthest away from the driver [2]. For example, v_{b1} (v_{f1}), v_{b2} (v_{f2}), ..., v_{bn} (v_{fn}) are the 1st, 2nd, ..., nth unit propagation TD of the near-end (far-end), respectively.

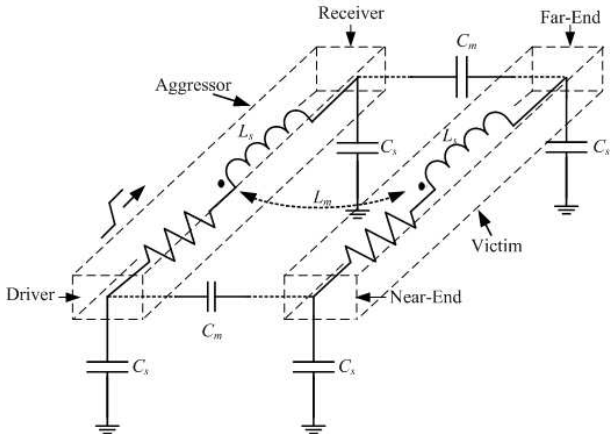

Figure 2. Equivalent model of a pair of transmission lines [1].

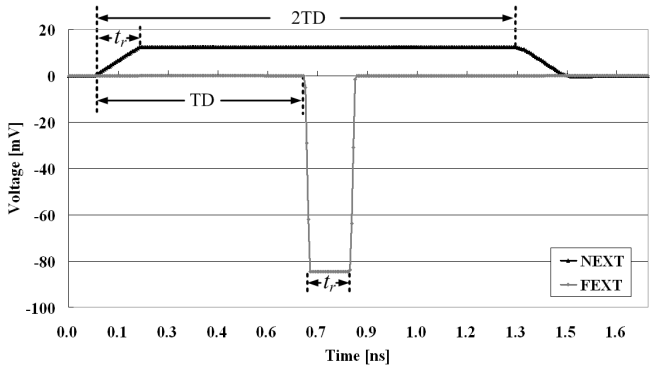

(a)

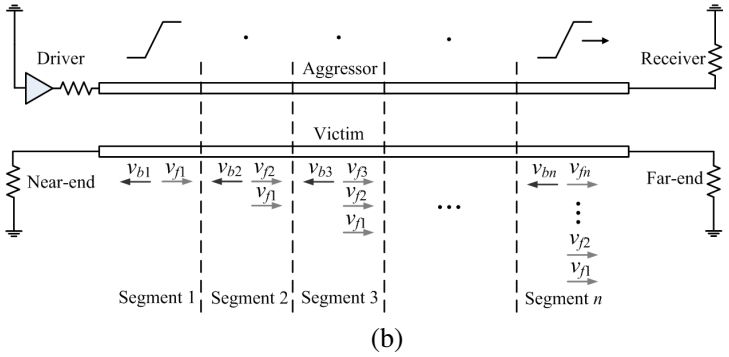

Figure 3. Schematic of typical crosstalk in a PCB. (a) Typical crosstalk signature of the victim without a guard trace [2, 6]. (b) Equivalent crosstalk behavior.

Since the signal state transients of the aggressor are transferred forward to the next unit, crosstalk also appears in the victim. The direction and propagation velocity of *FEXT* are the same as that of the signal of the aggressor. During the second state transient, v_{f2} overlaps v_{f1}, as shown in the second segment of Fig. 3(b). Finally, since all n previous *FEXT*s accumulate at segment n, as shown Fig. 3(a), the *FEXT* of segment n is greater than that of the previous segment $(n-1)$. Moreover, the holding time of *FEXT*, which is characterized by high amplitude, is equal to the rise time t_r of the pulse [2].

Since $NEXT_1$ (v_{b1}) can occur during the start of the signal state transient at the near end [2, 11], there is no accumulated phenomenon in the victim, as shown in the first segment of Fig. 3(a). Moreover, v_{bn}, which is induced by the aggressor at segment n, requires just one TD to arrive at the far end of the victim, as shown in segment n of Fig. 3(b). This v_{bn} also takes one more TD to arrive back at the near end (driver) of the victim. Therefore, the time of v_{bn} occurring at the near end of the victim is 2 TD. Since there is no accumulated phenomenon in the *NEXT* characteristics, its amplitude is lower than that of the *FEXT*, and the total holding time of the near-end pulse is 2 TD [2].

Once the overall crosstalk behavior is understood, the major effects can be analyzed separately with respect to C_m and L_m, and then merged into one. The crosstalk components of C_m and L_m were analyzed and derived as follows. The capacitive coupling equivalent circuit of C_m is shown in Fig. 4(a) [2, 12], assuming that there is only a capacitive effect between the two transmission lines. When the aggressor's state is transient, the coupling effect of the mutual capacitance transfers energy from the aggressor to the victim, both

of which have the same impedance. The induced noise from the aggressor is transmitted forward and backward to the near and far ends, respectively. Let i_{Cb} and i_{Cf} be the noise transmitted to the near and far ends, respectively, and i_{Cm} be the total induced noise from the aggressor due to this mutual capacitance, as shown in (1) and (2). Note that lowercase and capital letters designate one unit cell and the total amount of the current or voltage, respectively.

$$i_{Cm} = i_{Cb} + i_{Cf} \tag{1}$$

$$v_{Cf} = v_{Cb} \tag{2}$$

After getting the results of (1) and (2) and then deriving the voltage of the accumulated far-end crosstalk due to C_m, v_{CFEXT} is expressed and shown in (3) [12],

$$v_{CFEXT} = \frac{1}{2} Z_o C_m \zeta \frac{dv_s}{dt}. \tag{3}$$

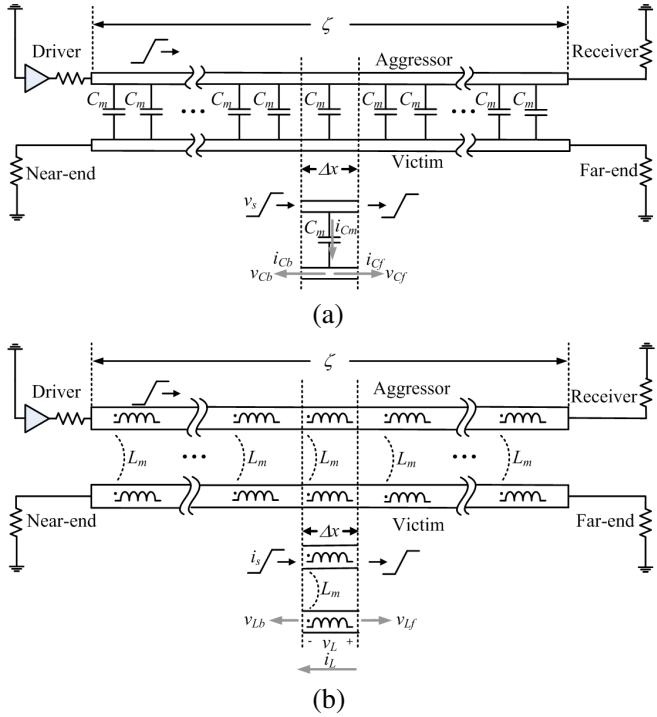

Figure 4. Equivalent circuit for crosstalk analysis for (a) capacitive coupling and (b) inductive coupling.

Let (dv_s/dt) be the instantaneous changing voltage, Z_o be the impedance of the transmission line, and ζ be the total effective coupling length [13].

Simultaneously, v_{CNEXT}, the near-end crosstalk due to C_m, is shown in (4) [12].

$$v_{CNEXT} = \frac{1}{4} Z_o C_m v_p v_o \tag{4}$$

Let v_p be the propagation velocity and v_o be the peak voltage [12].

The mutual inductance coupling equivalent circuit of L_m is shown in Fig. 4(b) [2, 12]. According to Lenz's law, an induced electromotive force will cause a current to flow in the closed loop in a direction that opposes the change in the linking magnetic flux [14]. Assuming that there is the only an inductive effect between the two transmission lines, there is an induced counter-electromotive force on the victim according to Lenz's law [14] when the aggressor's states are transient. Let v_L be the unit total induced noise from the aggressor due to this mutual inductance, as shown in (5) [12], where v_{Lb} and v_{Lf} are the unit induced backward and forward noises, respectively, of the opposing voltages, as shown in (6),

$$v_L = v_{Lb} - v_{Lf} \tag{5}$$

$$v_{Lb} = -v_{Lf} \tag{6}$$

After getting the results of (5) and (6) and then deriving the accumulated *FEXT* of the mutual inductance, v_{LFEXT} can be expressed and shown in (7) [12],

$$v_{LFEXT} = -\frac{1}{2} \frac{L_m \zeta}{Z_o} \frac{dv_s}{dt}. \tag{7}$$

Simultaneously, v_{LNEXT}, the *NEXT* of the mutual inductance, is shown in (8),

$$v_{LNEXT} = \frac{1}{4} \frac{L_m v_p v_o}{Z_o}. \tag{8}$$

The total crosstalk is the sum of the effects of the mutual capacitance and inductance in response to signal transients. Therefore, v_{FEXT} is the summation of (4) and (8) to give (9), and v_{NEXT} is the summation (3) and (7) to give (10) [12, 13].

$$v_{NEXT} = v_{CNEXT} + v_{LNEXT} = \frac{1}{4} v_p \left(Z_o C_m + \frac{L_m}{Z_o} \right) v_o \tag{9}$$

$$v_{FEXT} = v_{CFEXT} + v_{LFEXT} = \frac{1}{2} \zeta \left(Z_o C_m - \frac{L_m}{Z_o} \right) \frac{dv_s}{dt} \tag{10}$$

Since the guard trace can also decrease the coupling effect of the mutual capacitance and inductance here, the reduced ratio of the mutual inductance is more than that of the mutual capacitance. Therefore, such an effect can alleviate crosstalk [2, 10].

3. GUARD TRACE APPLICATION

Smaller separations between traces cause more mutual inductance and crosstalk, especially in high-density and high-speed PCB designs. Therefore, crosstalk will be an important criterion in the design of high-speed electronic products. Adding a guard trace between aggressor and victim traces can change the mutual coupling C_m and L_m to reduce crosstalk [10]. However, a single guard trace is also a potential noise source [2]. Therefore, if the guard trace is grounded, ideally to the absolute zero voltage, it may reduce noise by eliminating the interference between the aggressor and victim. Practical PCB designs cannot meet this grounding requirement, especially multi-layer PCB designs. Therefore, one complete layer usually serves as a ground plane and the other layers are signal trace planes. Generally, as many grounded vias as possible are included in designs, although this does not significantly improve the protection capability. Moreover, too many grounded vias reduce SI and introduce the side effects of parasitic capacity and inductance, which in turn influence protection capability [2, 8]. A design with not enough grounded vias will cause serious SI issues, as discussed below.

3.1. Effect of an Imperfect Guard Trace

Figure 5(a) shows the topology of a ground trace with two grounded vias. This is too few for an effective design [5, 6], and causes serious crosstalk, as shown in Fig. 5(d) [8]. Although the areas near the two grounded vias are grounded, the rest of the trace still acts as a transmission line with mutual coupling C_m and L_m between the aggressor and victim. Therefore, in the areas without grounded vias, the guard trace experiences crosstalk from the aggressor. In this situation, the noise in the guard trace becomes another noise source to interfere with the victim by way of the mutual coupling C_m and L_m between the guard trace and the victim [2, 8]. The typical crosstalk shown in Fig. 3(a) becomes the noise shown in Fig. 5(d), causing the *NEXT* and *FEXT* peak values to increase simultaneously.

The victim and the guard trace are affected by crosstalk from the transient states of the aggressor. *NEXT* and *FEXT* are generated in those areas of the guard trace without grounded vias, and the originally

neutral guard trace becomes another potential noise source to generate crosstalk, especially for high-amplitude *FEXT* [2, 8]. Falling-edge (high-to-low) and rising-edge (low-to-high) transients generate noise in the victim. There is no crosstalk effect to offer noise energy when the state of the guard trace returns to its original state. Therefore, the falling- and rising-edge transients cause positive and negative pulses, respectively, in the victim, as shown in Fig. 5(b). These induced two pulses overlap in *FEXT* in the victim to form the new *FEXT*, as shown in Fig. 5(d). Moreover, since there is no matched resistance on the guard trace, grounded vias are added to prevent noise [5, 6]. Reflection occurs in the guard trace according to reflection theorem, as shown in (11) [14], where Γ is the reflection coefficient, Z_L is the load impedance.

$$\Gamma = \frac{Z_L - Z_o}{Z_L + Z_o} \tag{11}$$

Let the impedance of the ideal grounded via be zero. Then, the impedance of the guard trace depends on the characteristic impedance Z_{trace}. When *FEXT* enters the grounded vias on the guard trace, the reflection coefficient Γ is -1, which means that the reflected and

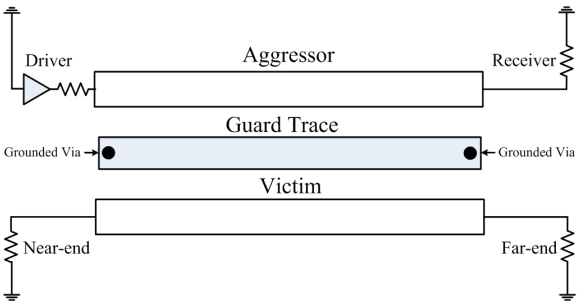

(a)

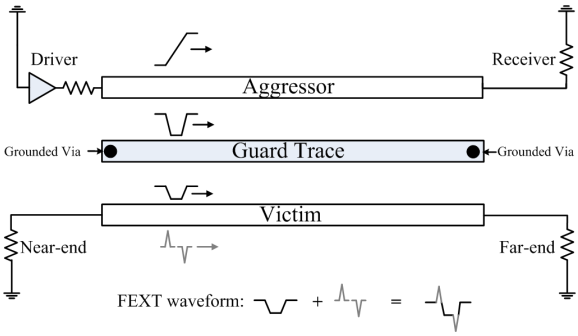

(b)

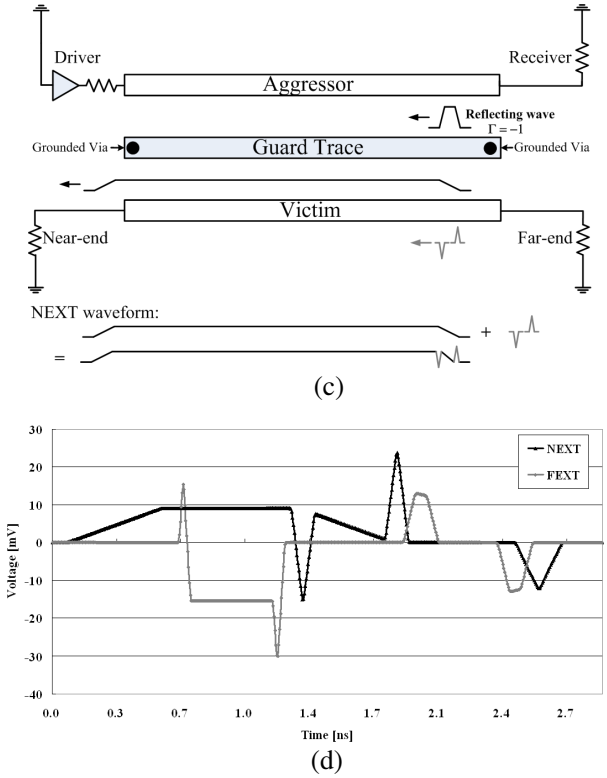

Figure 5. Crosstalk phenomenon caused by the guard trace and grounded vias. (a) Topology of the guard trace with two terminated grounded vias. (b) Phenomenon of repeating crosstalk caused by *FEXT* in the guard trace. (c) Crosstalk caused by grounded vias on the guard trace reflecting *FEXT*. (d) Simulation result of the guard trace with two terminated grounded vias [8].

incident waves have the opposite phase, since $Z_L = 0$ and $Z_o = Z_{trace}$ in (11). Therefore, *FEXT* in the guard trace is reflected forward to the near end, and this causes crosstalk in the victim. There are two *FEXT* transient states, and so there is *FEXT* in the victim, as shown in Fig. 5(c). Moreover, there are two positive and negative pulses back to the near end of the victim where they overlap; these are caused by reflections of *FEXT* in the guard trace [8, 14]. Therefore, positive and negative pulses at the near end enter the terminated resistor, as shown in Fig. 5(d). The near end of the guard trace still generates a reflection. Therefore, *FEXT* in the guard trace is continually travelling back and forth between the two grounded vias. Although too few

grounded vias in the guard trace can effectively reduce crosstalk from the aggressor, they themselves are the cause of more serious crosstalk from the guard trace because of the reflection that occurs, and this result in a more serious SI issue [2]. The aim of using the guard trace is to prevent, not increase, crosstalk. Thus, we propose a more suitable design methodology to minimize crosstalk in the victim while optimizing performance.

3.2. Effect of the Number of Grounded Vias on Guard Trace Performance

We have shown that too few grounded vias and unmatched impedance cause more crosstalk. To enhance crosstalk prevention, more grounded vias can be added to the guard trace. Consider the case where one more via is added, for a total of three, as shown in Fig. 6(a); the corresponding crosstalk is shown in Fig. 6(b). Compared with the crosstalk of the structure with two grounded vias shown in Fig. 5(d), it is clear that the *NEXT* pulses of the three-via structure occur earlier than in the two-via structure because of the middle grounded via. Therefore, *NEXT* in the victim with three grounded vias can appear as a first set of positive and negative pulses followed by a second set of pulses.

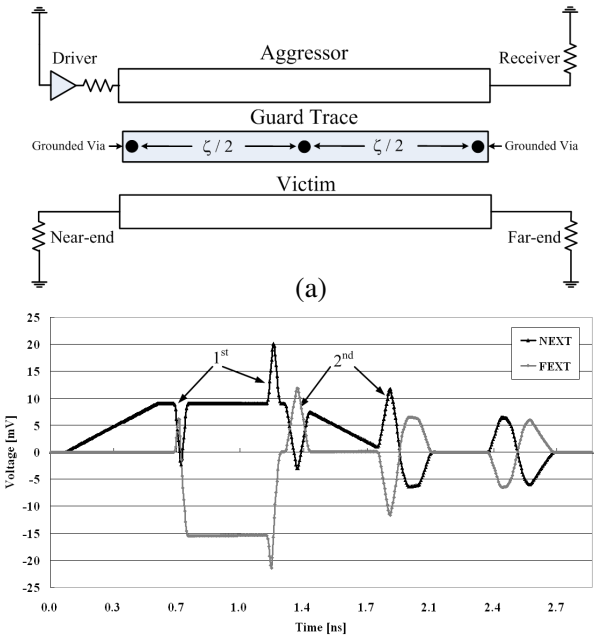

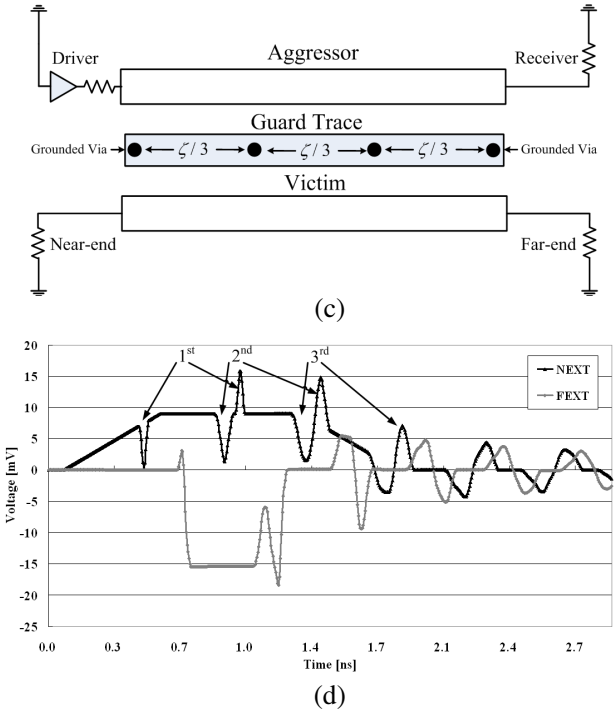

Figure 6. Guard trace with three and four grounded vias: (a) Simulated topology of the guard trace with three grounded vias, (b) simulation results of the structure in (a), (c) simulated topology of the guard trace with four grounded vias, and (d) simulation results of the structure in (c).

Next, consider the case with four grounded vias, two terminated vias, and two arithmetical-average grounded vias, as shown in Fig. 6(c); the corresponding performance is shown in Fig. 6(d). Compared with the three-via structure, *NEXT* pulses in the victim arrive earlier since they are reflected from the second grounded via. The negative pulse of the second set is ahead of the positive pulse of the first set, and the same is true of the subsequent pulses in order. Therefore, *NEXT* that causes negative and positive pulses in the victim changes according to the location of the grounded via. We can adjust the spacing of the grounded vias so that the first positive pulse cancels the second negative pulse. Therefore, this design can effectively eliminate the *NEXT* problem. Simultaneously in a similar way, the opposing *FEXT* pulses in the victim can offset each other. Since both *NEXT* and *FEXT*

are effectively reduced, the guard trace can provide optimal crosstalk prevention. Determining the appropriate locations of the grounded vias required to achieve this optimal performance of the guard trace is discussed later.

3.3. Proposed Design

Grounded vias in the guard trace can reduce the crosstalk that occurs due to transients in the aggressor. If we know the rise-time of the transient, we can calculate the distance (length of a segment) between grounded vias to achieve this, as shown in (12),

$$|Segment_{best}| = \frac{1}{2} \times v_p \times t_r \tag{12}$$

where $|Segment_{best}|$ is the optimal distance between two grounded vias and v_p is obtained from (13) [15],

$$v_p = \frac{3 \times 10^8}{\sqrt{\varepsilon_{reff}}}. \tag{13}$$

The speed of light is 3×10^8 m/s. Hence, ε_{reff} is the effective dielectric constant of the material, as shown in (14) [15],

$$\varepsilon_{reff} = \frac{\varepsilon_r + 1}{2}\left(1 + \frac{\varepsilon_r - 1}{\varepsilon_r + 1}\frac{\ln\frac{\pi}{2} + \frac{1}{\varepsilon_r}\ln\frac{4}{\pi}}{\ln\frac{8h}{w}}\right) \tag{14}$$

where ε_r, h, and w are the relative dielectric constant of the material, the thickness of the PCB, and the width of a microstrip [2, 10], respectively. The optimal location of grounded vias can be derived from (12). The optimal number of grounded vias, $|vias_{opt}|$, can be derived from (15),

$$|vias_{opt}| = \left\lceil \left| Length_{guard\text{-}trace} \right| / \left| Segment_{best} \right| \right\rceil + 1, \tag{15}$$

where $|Length_{guard-trace}|$ is the total length of the guard trace and $|vias_{opt}|$ is the number of grounded vias.

4. SIMULATION RESULTS

We used a simulation to confirm that the number and placement of grounded vias determined using our methodology generate the appropriate opposing pulses to reduce crosstalk. The simulation parameters were as follows: FR4 dielectric constant (ε_r) = 4.664,

thickness (h) = 13.87 mil, and microstrip width (w) = 25 mil. This implies that the characteristic impedance can controlled to less than $50 \pm 10\%\,\Omega$. In addition, the loss tangent was 0.035, the trace conductivity was 595,900 Ω/cm, and the length of the victim, guard trace, and aggressor were 4000 mil [16].

After obtaining v_p from (12), the above parameters were substituted into (13) and (14) to obtain $v_p = 6.358 \times 10^{12}$ mil/s. Then v_p and t_r were substituted into (15) to obtain $|Segment_{best}| = 1590$ mil. The optimal number of grounded vias was calculated to be 4 using $|Length_{guard\text{-}trace}| = 4000$ mil and $|Segment_{best}| = 1590$ mil in (15). The length of the final segment may be shorter than 1590 mil because the total length is not necessarily an even multiple of the segment lengths.

Table 1. Simulation results.

Simulation number	Number of grounded vias	|Segment| (mil)	*NEXT* peak (mV)	Reduced ratio of *NEXT* (%)	*FEXT* peak (mV)	Reduced ratio of *FEXT* (%)
1	NA (Note1)	(1-*W*)	57.98	84.39	−71.93	78.54
2	NA	(3-*W*)	12.51	27.65	−22.57	31.63
3	0	4000	35.29	74.35	− 36.6	57.84
4	2*	4000	23.76	61.91	−30.04	50.27
5	3*	2000	20.11	55	−21.44	28.03
6	4 (Basis)	1590	9.05	Basis	−15.43	Basis
7	4*	1333	15.85	42.90	−18.38	16.05
8	5*	1000	14.35	36.93	−17.07	9.60
9	6*	800	9.05	0	−15.43	0
10	7*	666	12.38	26.90	−16.55	6.77
11	8*	571	11.15	18.83	−16.01	3.62
12	9*	500	10.61	14.70	−15.43	0
13	10*	444	11.12	18.62	−15.96	3.32

Note 1: "NA" meanings not applicable [17].

Note 2: "*" is the arithmetic average distance, $|vias| = 1 + \lfloor |Length_{guard\text{-}trace}| / |Segment| \rfloor$.

Table 1 shows the results of simulations for 13 different conditions. The first (1-W [3]) was a simulation of a 25-mil space between the victim and aggressor with no guard trace. The second (3-W) was the same as the first, except that the space between the victim and aggressor was 75 mil. The 3-W ruler is first proposed and represented the approximate 70% flux boundary at logic current [3]. The third simulation was one guard trace without any grounded vias, and a 25-mil spaces between the aggressor, guard trace, and victim. The fourth and fifth simulations were similar to the third, but had two and three grounded vias, respectively. Our design method of calculating the optimal distance between two grounded vias was illustrated in the sixth simulation. There were four grounded vias placed at uniform distances in the seventh simulation. The remainder of the simulations consisted of between five and ten equally spaced grounded vias. In all cases, there was an impedance matching resistor on the aggressor and the victim, but not on the guard trace. The input clock parameters

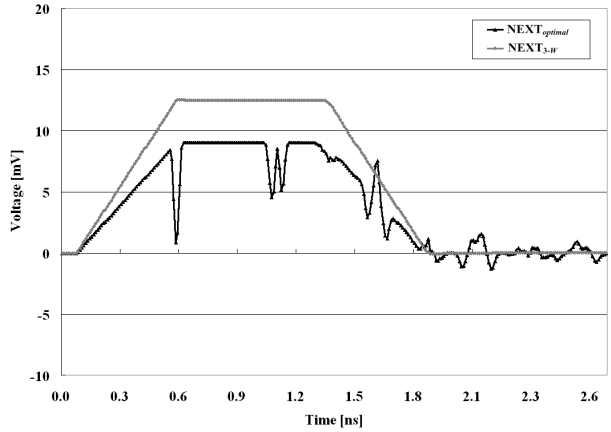

(a)

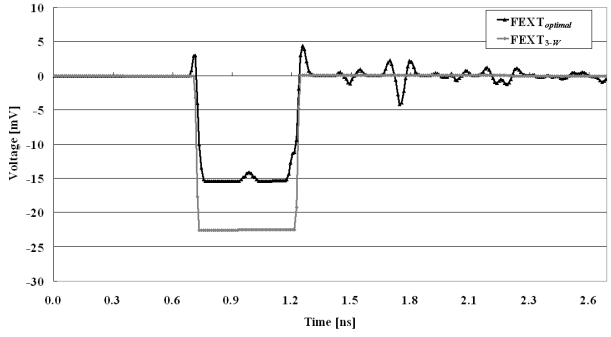

(b)

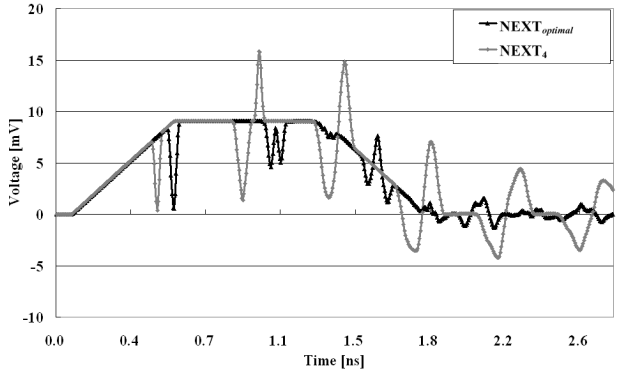

(c)

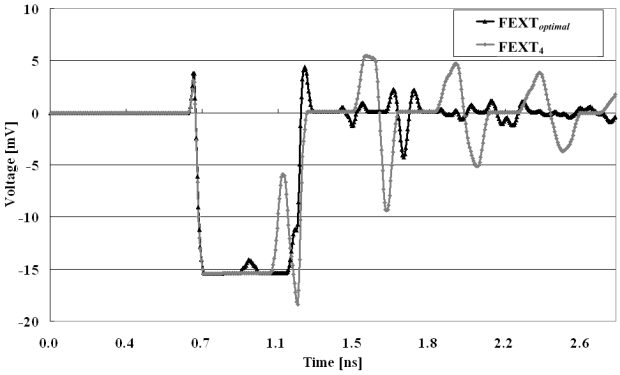

(d)

Figure 7. Comparisons of crosstalk simulation results with the optimal number of grounded vias calculated by the 3-W rule and arithmetic average method. (a) Example of $NEXT_{optimal}$ and $NEXT_{3\text{-}W}$. (b) Example of $FEXT_{optimal}$ and $FEXT_{3\text{-}W}$. (c) Example of $NEXT_{optimal}$ and $NEXT_4$. (d) Example of $FEXT_{optimal}$ and $FEXT_4$.

for the aggressor were an amplitude of 3.3 V, a frequency of 100 MHz, and a rise-time of 0.5 ns.

Figures 7(a) and (b) show that our 1590-mil model reduced *NEXT* and *FEXT* crosstalk by more than 26.62% and 31.06%, respectively compared with the 3-W rule [3]. Table 1 shows that compared to the situation of four (five) grounded vias at an average distance of 1333 (1000) mil, our proposed 1590-mil method reduced *NEXT* and *FEXT* crosstalk by more than 42.9% (36.3%) and 16.05% (9.6%), respectively. From above description, there is a fact that the crosstalk of the guard trace will be reflected back and forth constantly. Since the pulses of the victim are caused by the crosstalk and grounded via reflection

of the guard trace, these pulses of the victim will be also generated back and forth constantly. They will become the ringing noise, which is induced by the difference between capacitive and inductive coupling coefficients [8], as shown in Figs. 7(c) and (d). Then, Figs. 7(c) and (d) show that there are more amount of ringing noise happened at *NEXT* and *FEXT* in the structure of the arithmetic average distance with four grounded vias, respectively. Compared to the arithmetic average case, since the ringing noise of our design are offset by the negative pulses, as shown in Figs. 7(c) and (d), the ringing noise of our method is less than that of the arithmetic average design one. Therefore, our proposed approach not only can reduce the crosstalk but also alleviate the ringing noise caused by the crosstalk and the grounded vias reflection of the guard trace.

Moreover, the results of Table 1 show that an average distance of 800 mil gave the same performance as our optimal result. Since 800 mil is almost half our proposed distance of 1590 mil, this situation can also generate the opposing pulses required to reduce crosstalk. Although the performance was the same, almost twice the number of vias was required using the 800 mil distance. The number of grounded vias is shown in (16), where k is a positive integer. Here, $k = 1$ is the optimal performance such that the number of grounded vias is the minimum and the performance is optimal.

Table 2. PCB design parameters.

Parameter	Without guard trace		With guard trace				
	1	2	3	4	5	6	7
ε_r	4.664						
Loss tangent	0.035						
h (mil)	13.87						
t (mil)	0.7						
w (mil)	25						
s (mil)	25 (1-W)	75 (3-W)	25				
ζ (mil)	4000						
Z_o	50 Ω						
Number of grounded vias	NA		0	2*	4 (Basis)	4*	5*
|*Segment*| (mil)	NA		4000	4000	1590	1333	1000

$$|vias_{opt2}| = \left\lceil \left| Length_{guard\text{-}trace} \right| / (|Segment_{best}| / k) \right\rceil + 1 \qquad (16)$$

Let $NEXT_{optimal}$ ($FEXT_{optimal}$) and $NEXT_{3\text{-}W}$ ($FEXT_{3\text{-}W}$) be $NEXT$ ($FEXT$) of our proposed method and the 3-W rule, respectively. Let $NEXT_4$ ($FEXT_4$) be $NEXT$ ($FEXT$) of the arithmetic average design with four ground vias. In this study, there is no guard trace in the 1-W and 3-W rules, and the reduced crosstalk ratio is $((y\,\text{mV-}y$ "Basis" $\text{mV})/y\,\text{mV})\%$, where y "Basis" is the peak value of our proposed number of grounded vias with the optimal performance and y is the peak value of number of ground vias in all of other cases.

5. EXPERIMENTAL RESULTS

Our experimental structure was the same as the one simulated to confirm that our theoretical calculations were correct. The parameter set is shown in Table 2 and the simulation board topologies are shown in Figs. 8(a) and (b). There were seven PCB sets, exactly the same as the simulation structure.

Crosstalk in the victim was measured with an Agilent E8362B network analyzer in the frequency domain [5]. We obtained the time-domain information using a discrete Fourier transform [11]. Fig. 9 shows the physical PCB dimensions of our experimental board and Table 3 shows the experimental results. First, compared with the 3-W rule [3], our proposed approach not only reduced $NEXT$ and $FEXT$ by more than 34.49% and 37.55% over the time-domain as shown in Figs. 10(a) and (b), respectively, but also reduced down $NEXT$ and $FEXT$ by more than 2.1 dB and 3.3 dB over the frequency-domain before the first resonance with 2 GHz as shown in Figs. 10(c) and (d), respectively.

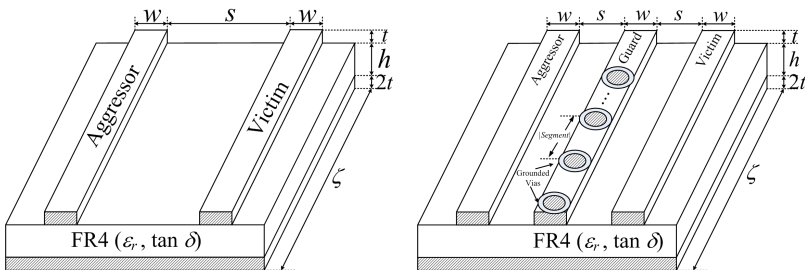

Figure 8. Board topology (a) without guard trace and (b) with guard trace.

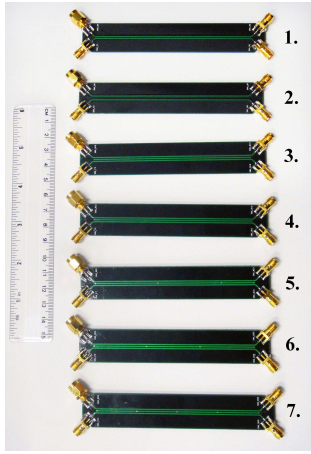

Figure 9. Experimental PCB measurement.

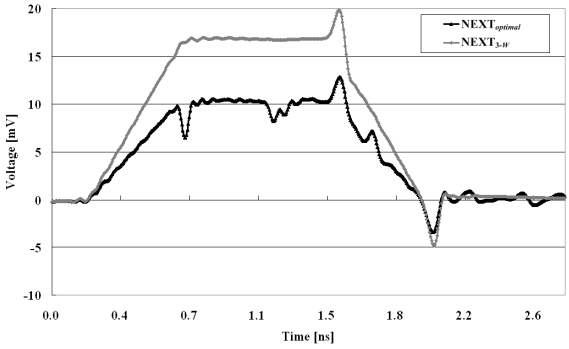

(a)

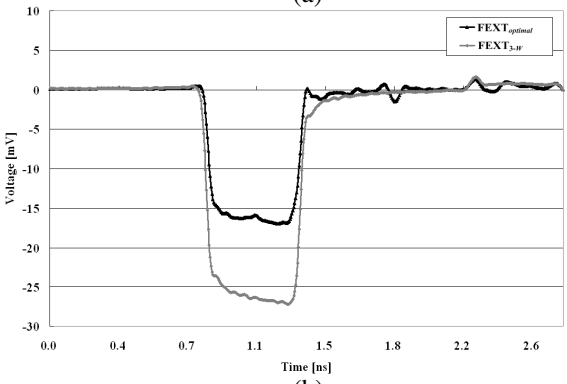

(b)

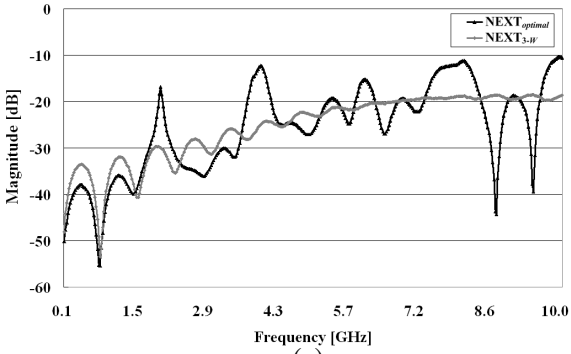

(c)

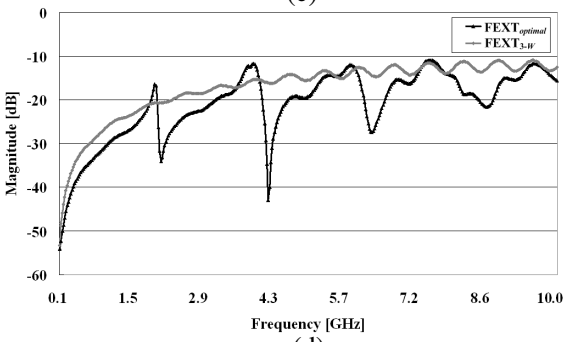

(d)

Figure 10. Comparison of experimental results for the optimal number grounded vias and the design according to the 3-W rule. (a) Example of $FEXT_{optimal}$ and $FEXT_{3\text{-}W}$ over time-domain. (b) Example of $FEXT_{optimal}$ and $FEXT_{3\text{-}W}$ over time-domain. (c) Example of $FEXT_{optimal}$ and $FEXT_{3\text{-}W}$ over frequency-domain. (d) Example of $FEXT_{optimal}$ and $FEXT_{3\text{-}W}$ over frequency-domain.

Moreover, compared to the other methods, our method changed the pulse position in the victim by selecting the proper segment distance in the guard trace so that the negative pulses canceled the positive pulses to reduce the crosstalk. Hence, compared with the arithmetic average method, our approach reduced *NEXT* and *FEXT* by more than 20.94% and 0.88% over the time-domain as shown in Figs. 11(a) and (b), respectively, although the performance between them is roughly the same over the frequency-domain with the different resonances as shown in Figs. 11(c) and (d), respectively. Therefore, our proposed approach can get the more performance than other methods over the time-domain although the performance between them is roughly the same before the first resonance frequency-domain.

From the results, if the first appearance of resonance design is

Table 3. Experimental results.

Number of grounded vias	Segment length (mil)	*NEXT* peak (mV)	Improved ratio of *NEXT* (%)	*FEXT* peak (mV)	Improved ratio of *FEXT* (%)
NA	1-*W*	80.7	84.09	−66.79	74.58
NA	3-*W*	19.6	34.49	−27.19	37.55
0	4000	28.4	54.79	−29.5	42.44
2*	4000	12.96	0.93	−18.62	8.81
4 (Basis)	1590	12.84	Basis	−16.98	Basis
4 *	1333	16.24	20.94	−17.13	0.88
5*	1000	13.35	3.82	−17.3	1.85

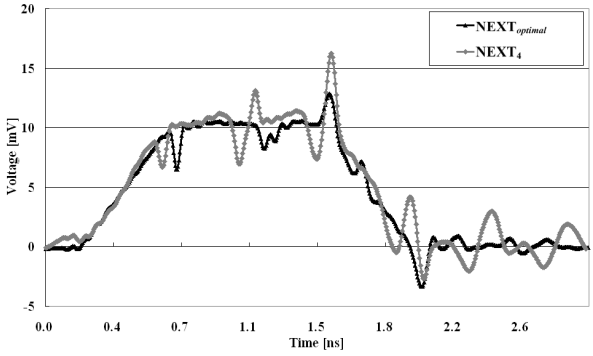

(a)

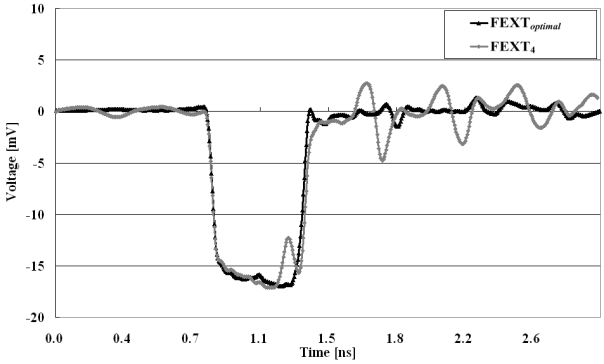

(b)

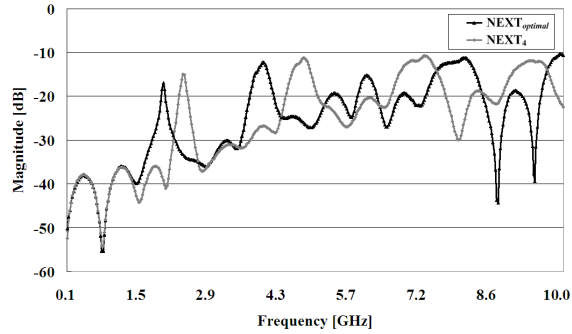

(c)

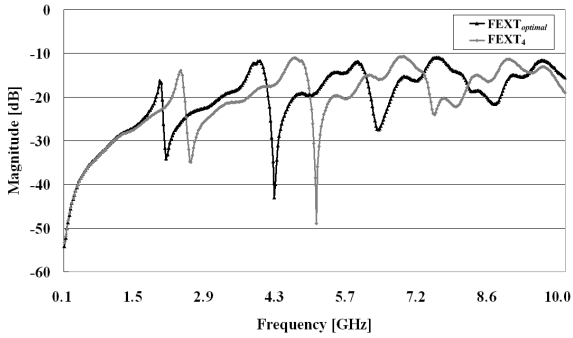

(d)

Figure 11. Comparison of experimental results for the optimal number grounded vias and the design according the arithmetic average method. (a) Example of $FEXT_{optimal}$ and $FEXT_4$ over time-domain. (b) Example of $FEXT_{optimal}$ and $FEXT_4$ over time-domain. (c) Example of $FEXT_{optimal}$ and $FEXT_4$ over frequency-domain. (d) Example of $FEXT_{optimal}$ and $FEXT_4$ over frequency-domain.

2 GHz, our proposed structure can get the smallest number of vias required to achieve optimal performance in reducing crosstalk over the time-domain and frequency-domain. Additionally, a wider bandwidth of one design can be obtained by shortening the distance between two grounded vias which makes the first resonance to be extended to the high frequency [5, 8]. Finally, apply the Equation (16) of our proposed approach to adjust the distance between two grounded vias for a wider bandwidth design. Our proposed structure can get the smallest number of vias required to achieve optimal performance in reducing crosstalk over the time and before the first resonance frequency-domain.

In the experiment case, the amount of the ringing noise has been decreased in our approach, since it is the same reason with

the simulation case. Therefore, the ringing noise can be alleviated in our approach, as shown in Figs. 11(a) and (b), respectively. Finally, the simulation and experiment results indicate that our proposed approach can simultaneously and effectively alleviate the crosstalk and the ringing noise.

6. DISCUSSION

Our measurement results demonstrate that our theoretical model is capable of preventing crosstalk and achieving maximum efficiency. The comparisons of *NEXT* and *FEXT* for the simulation and experimental results in our design are shown in Figs. 12(a) and (b). The simulation results have good consistency with that of experiment measurement. Hence, this can show that our proposed results are correct. Moreover, since the connector of the measurement instrument and welds will cause the impedance mismatch, there is an error between them. It can be shown and measured by time-domain reflectometer (TDR). The output signal was 200 mV and the rise-time of the step function was 50 ps. The near and far ends of the victim were terminated by 50-Ω resistors to avoid crosstalk caused by reflection. An Agilent 86100C TDR was used measure the impedance change of our PCB design and showed a pulse occurring at 1.5 ns that did not occur in the simulation; this was due to the impedance mismatch between the subminiature type-A (SMA) connector and the pad as shown in Fig. 12(c). Although this mismatch caused some discrepancy between the simulation and experimental measurement results, we know from our experimental results that our proposed model can achieve a certain improvement rate. If the impedance between the connector and pad could be matched, there would be no pulse at 1.5 ns and the level of improvement would be even greater. Figs. 10(a) and 11(a) shows that the positive and negative pulses can be merged into one to offset the peak noise value if the grounded vias are located according to our design.

The common and differential modes can be simultaneously excited during the crosstalk. Since these two modes will respectively increase and decrease the characteristic impedance [11], the trace impedance will be changed during the crosstalk. Therefore, there is an error in the measurement, since the impedance of the measurement instrument cannot be well matched with the trace. Although there is the error between the simulation and measurement, our proposed approach still owns the best capability to reduce the crosstalk and the ringing noise. Thus, our proposed methodology provides the fewest grounded vias required to achieve the optimal performance and reduce crosstalk.

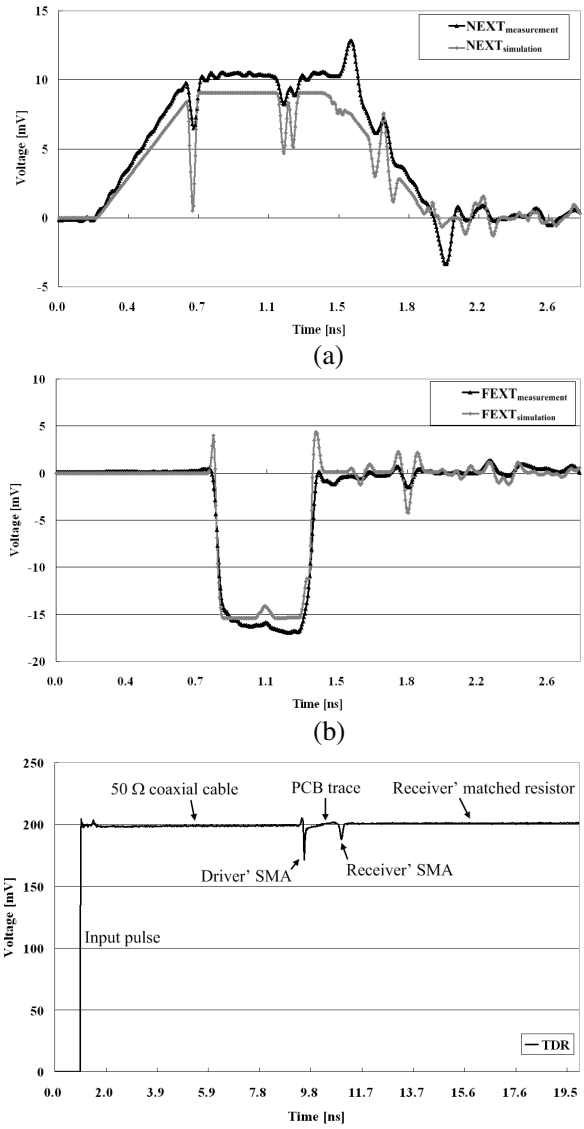

Figure 12. (a) Comparison of *NEXT* for the simulation and experiment results. (b) Comparison of *FEXT* for the simulation and experiment results. (c) Unmatched impedance of the PCB experiments indicated by the TDR measurement.

7. CONCLUSION

We proposed a method to calculate the optimal number of grounded vias required to prevent crosstalk and obtain the maximum efficiency. The proper segment distance of the guard trace calculated by our method can change the position of a pulse in the victim so that a negative pulse offsets a positive one. These two opposite pulses cancel each other and reduce crosstalk. The optimal performance predicted by our proposed theoretical model was confirmed by consistent simulation and experimental results. We showed that our method reduced *NEXT* and *FEXT* by more than 27.65% and 31.63% using time-domain simulation, respectively. Moreover, we showed that our method reduced *NEXT* and *FEXT* by more than 34.49% (2.1 dB) and 37.55% (3.3 dB) using time-domain (frequency-domain) experiment, respectively. Simultaneously, the ringing noise can be alleviated by a negative pulse to offset a positive one in our approach such that it can reduce the amount of the ringing noise caused by the crosstalk and grounded vias reflection of the guard trace. Moreover, our results infer that fewer properly grounded vias produce optimal performance, increase available layout space, increase SI, and decrease physical fragility without adding another potential noise source.

ACKNOWLEDGMENT

The authors would like to thank the National Science Council of the Republic of China for financially supporting this research under Contract No. NSC 97-2218-E-159-002- and NSC 97-2622-E-027-009-CC3.

REFERENCES

1. Sharawi, M. S., "Practical issues in high speed PCB design," *IEEE Potentials*, Vol. 23, No. 2, 24–27, Apr./May 2004.
2. Bogatin, E., *Signal Integrity-simplified*, Prentice Hall, 2003.
3. Montrose, M. I., *EMC and the Printed Circuit Board: Design, Theory, and Layout Made Simple*, IEEE Press, 1998.
4. Rossi, D., P. Angelini, C. Metra, G. Campardo, and G. Vanalli, "Risks for signal integrity in system in package and possible remedies," *13th IEEE European Test*, 165–170, May 2008.
5. Novak, I., B. Eged, and L. Hatvani, "Measurement by vector-network analyzer and simulation of crosstalk reduction on printed board with additional center traces," *IEEE Institute of Technology Conference*, 269–274, Irvine, CA, 1993.

6. Novak, I., B. Eged, and L. Hatvani, "Measurement and simulation of crosstalk reduction by discrete discontinuities along coupled PCB traces," *IEEE Transactions on Instrumentation and Measurement*, Vol. 43, No. 2, 170–175, Apr. 1994.
7. Ladd, D. N. and G. Costache, "SPICE simulation used to characterize the cross-talk reduction effect of additional tracks grounded with vias on printed circuit boards," *IEEE Transaction on Circuits and Systems II*, Vol. 39, 342–347, Jun. 1992.
8. Cheng, Y. S., W. D. Guo, G. H. Shine, H. H. Cheng, C. C. Wang, and R. B. Wu, "Fewest vias design for microstrip guard trace by using overlying dielectric," *IEEE Electrical Performance of Electronic Packaging*, 321–324, Oct. 2008.
9. Suntives, A., A. Khajooeizadeh, and R. Abhari, "Using via fences for crosstalk reduction in PCB circuits," *IEEE International Symposium on Electromagnetic Compatibility*, Vol. 1, 34–37, Aug. 2006.
10. Lee, K., H. B. Lee, H. K. Jung, J. Y. Sim, and H. J. Park, "A serpentine guard trace to reduce the far-end crosstalk voltage and the crosstalk induced timing jitter of parallel microstrip lines," *IEEE Transactions on Advanced Packaging*, Vol. 31, No. 4, 809–817, Nov. 2008.
11. Hall, S. H., G. W. Hall, and J. A. McCall, *High-speed Digital System Design: A Handbook of Interconnect Theory and Design Practices*, John-Wiley & Sons, 2000.
12. Young, B., *Digital Signal Integrity: Modeling and Simulations with Interconnects and Packages*, Prentice-Hall, 2001.
13. Muthana, P. and H. Kroger, "Behavior of short pulses on tightly coupled microstrip lines and reduction of crosstalk by using overlying dielectric," *IEEE Transactions on Advanced Packaging*, Vol. 30, No. 3, 511–520, Aug. 2007.
14. Cheng, D. K., *Field and Wave Electromagnetics*, 2nd edition, Addison-Wesley, 1989.
15. Sobol, H., "Applications of integrated circuit technology to microwave frequencies," *Proceedings of the IEEE*, 1200–1211, Aug. 1971.
16. Advance Allegro PCB SI Techniques V15.2, *Cadence*, 2005.
17. Mbairi, F. D., W. P. Siebert, and H. Hesselbom, "On the problem of using guard traces for high frequency differential lines crosstalk reduction," *IEEE Transactions on Components and Packaging Technologies*, Vol. 30, No. 1, 67–74, Mar. 2007.